

Multi-Scored Sleep Databases: How to Exploit the Multiple-Labels in Automated Sleep Scoring

Luigi Fiorillo^{1,2,*;†}, Davide Pedroncelli^{3;†}, Valentina Agostini³,
Paolo Favaro¹ and Francesca Dalia Faraci²

¹Institute of Informatics, University of Bern, Bern, Switzerland, ²Institute of Digital Technologies for Personalized Healthcare (MeDiTech), Department of Innovative Technologies, University of Applied Sciences and Arts of Southern Switzerland, Lugano, Switzerland, ³Department of Electronics and Telecommunications, Politecnico di Torino, Torino, Italy.

Institution where work was performed: Institute of Digital Technologies for Personalized Healthcare (MeDiTech), Department of Innovative Technologies, University of Applied Sciences and Arts of Southern Switzerland, Lugano, Switzerland.

†These authors contributed equally to this work.

*Corresponding author. Luigi Fiorillo, Institute of Digital Technologies for Personalized Healthcare (MeDiTech), Department of Innovative Technologies, University of Applied Sciences and Arts of Southern Switzerland, Lugano, Switzerland. Email:

luigi.fiorillo@supsi.ch.

Abstract

Study Objectives: Inter-scorer variability in scoring polysomnograms is a well-known problem. Most of the existing automated sleep scoring systems are trained using labels annotated by a single scorer, whose subjective evaluation is transferred to the model. When annotations from two or more scorers are available, the scoring models are usually trained on the scorer consensus. The averaged scorer's subjectivity is transferred into the model, losing information about the internal variability among different scorers. In this study, we aim to insert the multiple-knowledge of the different physicians into the training procedure. The goal is to optimize a model training, exploiting the full information that can be extracted from the consensus of a group of scorers.

Methods: We train two lightweight deep learning based models on three different multi-scored databases. We exploit the label smoothing technique together with a soft-consensus (LS_{SC}) distribution to insert the multiple-knowledge in the training procedure of the model. We introduce the averaged cosine similarity metric (ACS) to quantify the similarity between the hypnodensity-graph generated by the models with- LS_{SC} and the hypnodensity-graph generated by the scorer consensus.

Results: The performance of the models improves on all the databases when we train the models with our LS_{SC} . We found an increase in ACS (up to 6.4%) between the hypnodensity-graph generated by the models trained with- LS_{SC} and the hypnodensity-graph generated by the consensus.

Conclusions: Our approach definitely enables a model to better adapt to the consensus of the group of scorers. Future work will focus on further investigations on different scoring architectures.

Keywords: automatic sleep stage classification, machine learning, deep learning, multi-scored sleep databases.

Statement of Significance

Visual scoring of polysomnography is a highly subjective procedure. Several studies consistently reported the poor agreement between different physicians scoring the same whole-night recording. Existing sleep scoring algorithms, trained on multi-scored databases, overlook to encode in their models the variability among the scorers. We propose a technique to wholly insert the multiple-knowledge of the different physicians into the training procedure of a scoring algorithm. Our approach enables the model to better adapt to the consensus of the group of scorers. Whenever multi-scored databases are available, future researchers should train their models considering the annotations of all the physicians at the same time, rather than averaging their labels and training their algorithm on the averaged consensus.

Introduction

Sleep disorders represent a significant public health problem that affects millions of people worldwide [1]. Since the late 1950s, the polysomnography (PSG) exam has been the gold standard to study sleep and to identify sleep disorders. It monitors electrophysiological signals such as electroencephalogram (EEG), electrooculogram (EOG), electromyogram (EMG) and electrocardiogram (ECG). The physicians visually extract sleep cycle information from these signals. The whole-night recording is divided in 30-second epochs, and each epoch is classified into one of the five sleep stages (i.e. wakefulness W, stage N1, stage N2, stage N3, and stage REM) according to the AASM guidelines [2]. Worst case scenario, an eight-hour PSG may require up to two hours of tedious repetitive and time-consuming work to be scored. In addition, this manual procedure is highly affected by a low inter-rater scoring agreement (i.e. the agreement between different physicians scoring the same whole-night recording). The inter-rater scoring agreement value ranges from 70% up to slightly more than 80% [3-5]. In [3] the averaged inter-rater agreement of about 83% results from a study conducted on the AASM Inter-scorer reliability dataset, by using sleep stages annotated from more than 2,500 sleep scorers. The agreement was higher than 84% for awake, N2 and REM stages, but it dropped to 63% and 67% for N1 and N3 stages respectively. In fact, the inter-rater agreement varies among sleep stages, patients, sleep disorders and across sleep centers [3], [6].

Since 1960 many different approaches and algorithms have been proposed to automate this time-consuming scoring procedure. Mainly, two different approaches emerged: sleep scoring algorithms learning from well defined features extracted from the knowledge of the experts (shallow learning), and sleep scoring algorithms learning directly from the raw data (deep learning). Thorough reviews about feature based [7-8] and deep learning based [9-10] sleep scoring algorithms can be found in literature. Although the latter algorithms emerged only five years ago, their impressive results have never been reached with the previous conventional feature based approaches. Autoencoders [11], deep neural networks [12],

convolutional neural networks [13-20], recurrent neural networks [21-23] and different combinations of them [24-30] have been all proposed only in these last five years.

Almost all of the above algorithms have been trained on recordings scored by a single expert physician. The first remarkable exception comes from [27], where they consider recordings scored by six different physicians [31]. The scoring algorithm was trained on the six-scorer consensus (i.e. based on the majority vote weighted by the degree of consensus from each physician). In [23] the *Dreem* group introduced two publicly-available datasets scored by five sleep physicians. Similarly, they used the scorer consensus to train their automated scoring system. It has been shown that the performance of an automated sleep scoring system is on-par with the scorer consensus [23,27], and mainly that their best scoring algorithm is better than the best human scorer - i.e. the scorer with the higher consensus among all the physicians in the group. Although they both considered the knowledge from the multiple scorers - by averaging their labels and by training their algorithm on the averaged consensus - they still trained the algorithm on a single one-hot encoded label. Indirectly, they are still transferring the best scorer's subjectivity into the model, and they are not explicitly training the model to adapt to the consensus of the group of scorers.

In this work, we train two existing lightweight deep learning-based sleep staging algorithms, our DeepSleepNet-Lite [32] and SimpleSleepNet [23], on three open-access multi-scored sleep datasets. We consider the multiple-labels in the training procedure, i.e. the annotations of all the physicians are taken into account at the same time.

First we assess the performance of both scoring systems trained with the scorer consensus, and compare it to the performance of the individual scorer-experts. Then we exploit label smoothing along with the *Soft – Consensus* distribution to insert the multiple-knowledge into the training procedure of the models and to better calibrate the scoring architectures. We quantify the similarity between the hypnodensity-graph generated by the models - trained with and without label smoothing - and the hypnodensity-graph generated by the scorer consensus. We finally further analyze the ability of the uncertainty estimate and query procedure, proposed in [32], to identify the most challenging sleep stage predictions on our

calibrated DeepSleepNet-Lite, on both the model trained with and without smoothing their labels, whilst using a *Soft – Consensus* distribution. We aim at exploring if with a better calibrated model (*i.e.*, the predicted probability value \hat{p} mirrors its ground truth correctness likelihood) we are able to detect a higher number of misclassified epochs.

In the present work we investigate a different approach in exploiting multi-scored database information. In particular: (1) we demonstrate the efficiency of label smoothing along with the *Soft – Consensus* distribution in both calibrating and enhancing the performance of both DeepSleepNet-Lite and SimpleSleepNet; (2) we show how the model can better resemble the scorer group consensus, leading to a similarity increase between the hypnodensity-graph generated by the model and the hypnodensity-graph generated by the scorer consensus; (3) we prove the efficiency of the query procedure in detecting the most challenging sleep epochs, and we found that with a better calibrated model we are not always able to better detect the misclassified epochs.

Methods

Datasets

In this study we use the two publicly available databases introduced in [23] DOD-H (Dreem Open Dataset - Healthy) and DOD-O (Dreem Open Dataset - Obstructive), and the IS-RC (Inter-scorer Reliability Cohort) introduced in [31] to assess the inter-scorer reliability among different sleep centers.

IS-RC. The dataset contains 70 recordings (0 males and 70 females) from patients with sleep-disordered breathing aged from 40 to 57. The recordings were collected at the University of Pennsylvania. Each recording includes the EEG derivations C3-M2, C4-M1, O1-M2, O2-M1, one EMG channel, left/right EOG channels, one ECG channel, nasal airway

pressure, oronasal thermistor, body position, oxygen saturation and abdominal excursion.

The recordings are sampled at 128 Hz.

We only consider the single-channel EEG C4-M1 to train our DeepSleepNet-Lite architecture, and we use multi-channel EEG, EOG, EMG and ECG to train the SimpleSleepNet architecture. A band-pass Chebyshev IIR filter is applied between [0.3, 35] Hz. Each recording is scored by six clinicians from five different sleep centers (i.e. University of Pennsylvania, University of Wisconsin at Madison, St. Luke's Hospital (Chesterfield), Stanford University and Harvard University) according to the AASM rules [2].

The dataset contains the following annotations W , $N1$, $N2$, $N3$, R , and NC , where NC is a not classified epoch. Some epochs are not scored by all the six physicians, and even for some of them we don't have any annotation (i.e. NC). We decided to remove the epochs classified by all the scorers as NC . Epochs with less than six annotations are equally taken into account to avoid excessive data loss.

DOD-H. The dataset contains 25 recordings (19 males and 6 females) from healthy adult volunteers aged from 18 to 65 years. The recordings were collected at the French Armed Forces Biomedical Research Institute's (IRBA) Fatigue and Vigilance Unit (Bretigny-Sur-Orge, France). Each recording includes the EEG derivations C3-M2, C4-M1, F3-F4, F3-M2, F3-O1, F4-O2, O1-M2, O2-M1, one EMG channel, left/right EOG channels and one ECG channel. The recordings are sampled at 512 Hz.

DOD-O. The dataset contains 55 recordings (35 males and 20 females) from patients suffering from obstructive sleep apnea (OSA) aged from 39 to 62 years. The recordings were collected at the Stanford Sleep Medicine Center. Each recording includes the EEG derivations C3-M2, C4-M1, F4-M1, F3-F4, F3-M2, F3-O1, F4-O2, FP1-F3, FP1-M2, FP1-O1, FP2-F4, FP2-M1, FP2-O2, one EMG channel, left/right EOG channels and one ECG channel. The recordings are sampled at 250 Hz.

We only consider the single-channel EEG C4-M1 to train our DeepSleepNet-Lite architecture, and we use all the available channels to train SimpleSleepNet architecture, on both DOD-H and DOD-O. As in [23], a band-pass Butterworth IIR filter is applied between

[0.4, 18] Hz to remove residual PSG noise, and the signals are resampled at 100 Hz. The signals are then clipped and divided by 500 to remove extreme values. The recordings from both DOD-H and DOD-O datasets are scored by five physicians from three different sleep centers according to the AASM rules [2].

DOD-H and DOD-O contain the following annotations W , $N1$, $N2$, $N3$, R , and NC , where NC is a not classified epoch. All the scorers agree about the NC epochs (100% of agreement). Therefore, all of them are removed from the data. Unlike the previous IS-RC database, for each epoch five annotations are always available.

In [Table 1](#) we report a summary of the total number and percentage of the epochs per sleep stage for the DOD-H, DOD-O and IS-RC datasets.

Consensus in the multi-scored datasets

Inspired by [23,27], we evaluate the performance of the sleep scoring architectures, as well as the performance of each physician, using the consensus among the five/six different scorers. The majority vote from the scorers has been computed - i.e. we assign to each 30-second epoch the most voted sleep stage among the physicians. In case of ties, we consider the label from the most reliable scorer. The most reliable scorer is the one that is frequently in agreement with all the others. We use the *Soft-Agreement* metric proposed in [23] to rank the reliability of each physician, and to finally define the most reliable scorer. We denote with J the total number of scorers and with j the single-scorer. The one-hot encoded sleep stages given by the scorer j are: $\hat{y}_j \in [0, 1]^{K \times T}$, where K is the number of classes, i.e.

$K = 5$ sleep stages, and T is the total number of epochs. The probabilistic consensus \hat{z}_j among the $J - 1$ scorers (j excluded) is computed using the following:

$$\hat{z}_j = \frac{\sum_{i=1}^J \hat{y}_i[t]}{\max_{i=1}^J \sum_{i=1}^J \hat{y}_i[t]} \quad \forall t; \quad i \neq j \quad (1)$$

where t is the t -th epoch of T epochs and $\hat{z}_j \in [0, 1]^{K \times T}$, i.e. 1 is assigned to a stage if it matches the majority or if it is involved in a tie. The *Soft-Agreement* is then computed across all the T epochs as:

$$\text{Soft-Agreement}_j = \frac{1}{T} \sum_{t=0}^T \hat{z}_j[y_j] \quad (2)$$

where $\hat{z}_j[y_j]$ denotes the probabilistic consensus of the sleep stage chosen by the scorer j for the t -th epoch. $\text{Soft-Agreement}_j \in [0, 1]$, where the zero value is assigned if the scorer j systematically scores all the annotations incorrectly compared to the others, whilst 1 is assigned if the scorer j is always involved in tie cases or in the majority vote. The *Soft-Agreement* is computed for all the scorers, and the values are sorted from the highest - high reliability - to the lowest - low reliability. The *Soft-Agreement* is computed for each patient, i.e. the scorers are ranked for each patient, and in case of a tie the top-1 physician will be the one used for that patient.

Deep learning-based scoring architectures

We run our experiments on both DeepSleepNet-Lite architecture [32] and SimpleSleepNet architectures [23].

DeepSleepNet-Lite (DSN-L) [32] is a simplified *feed-forward* version of the original DeepSleepNet by [24]. Unlike the original network, in [32] we proposed to employ only the first *representation learning* block, and we proposed to simply train it with a *sequence-to-epoch* learning approach. Thus, the architecture receives in input a sequence of 90-second epochs, and it predicts the corresponding target of the central epoch of the sequence $x(t)$.

The *representation learning* architecture consists of two parallel CNNs branches, with small $CNN_{\theta_{Small}}$ and large $CNN_{\theta_{Large}}$ filters at the first layer. The principle is to extract high-time

resolution patterns with the small filters, and to extract high-frequency resolution patterns with the large ones. This idea comes from the way the signal processing experts define the trade-off between temporal and frequency precision in the feature extraction procedure [33]. Each CNN branch consists of four convolutional layers and two max-pooling layers. Each convolutional layer executes three basic operations: 1-D convolution of the filters with the sequential input; batch normalization [34]; element-wise rectified linear unit (ReLU) activation function. Then the pooling layers are used to downsample the input. In [Figure 1](#) we report an overview of the architecture, with details about the filter size, the number of filters and the stride size of each convolutional layer. The pooling size and the stride size for each pooling layer are also specified.

The convolutional neural networks $CNN_{\theta_{Small}}$ and $CNN_{\theta_{Large}}$ take as input the 90-second single-channel EEG \bar{x}_i signal. The parameters θ of the CNNs are independently trained so as to output the two encoding feature vectors \bar{h}_i^S (3) and \bar{h}_i^L (4). The two vectors are then concatenated in \bar{f}_i , (5) and forwarded to the final *softmax* layer.

$$\bar{h}_i^S = CNN_{\theta_{Small}}(\bar{x}_i) \quad (3)$$

$$\bar{h}_i^L = CNN_{\theta_{Large}}(\bar{x}_i) \quad (4)$$

$$\bar{f}_i = \bar{h}_i^S \parallel \bar{h}_i^L \quad (5)$$

The *softmax* function (6-7), together with the cross-entropy loss function (8), is used to train the model to output the logits \bar{z}_i and the final probabilities of the five mutually exclusive sleep stages classes.

$$\bar{z}_i = W^T \bar{f}_i + \bar{b} \quad (6)$$

$$\hat{p}_{i,k} = \frac{\exp(z_{i,k})}{\sum_j \exp(z_{i,j})} \quad (7)$$

$$H(\bar{y}_i, \bar{p}_i) = \sum_{k=1}^K -y_{i,k} \cdot \log(\hat{p}_{i,k}) \quad (8)$$

where $\theta = \{W, \bar{b}\}$ are the parameters of the *softmax* layer, j is the index of the vector \bar{z} , $\hat{p}_{i,k}$ is the output probability of class k of $x(t)$, i.e. the centered 30-second signal in \bar{x}_i . In (8) we compute the cross-entropy loss to quantify the agreement between the prediction \bar{p}_i and the target \bar{y}_i (i.e. sleep stage label).

SimpleSleepNet (SSN) [23] consists of two main parts as shown in Figure 2. The first part of the architecture is inspired by [22], whilst the second part that devises the sequence dependencies, is inspired by [24].

The *epoch encoder* part, or what we refer to as epoch processing block (*EPB*), is designed to process 30-second multi-channel EEG epochs, and it aims at learning epoch-wise features. The *EPB* block consists of four modules: (1) spectrogram, (2) signals and frequencies reduction, (3) GRU with attention and (4) positional embedding. In (1) the short-term Fourier transform is computed on each preprocessed epoch, resulting in a time-frequency image $S \in \mathfrak{R}^{C,T,N}$, where C is the number of channels, T is the number of time-steps and N the number of frequency bins. In (2) independent linear projections are applied on the frequencies and channels/signals axis to project $\mathfrak{R}^{C,T,N}$ into $\mathfrak{R}^{c,T,n}$, where $c \leq C$ and $n \leq N$ are the linearly reduced channels and frequencies respectively. In (3) the reshaped $\mathfrak{R}^{T,c,n}$ is the input of the GRU block and the attention layer (implemented as in [35]), and the output is the representation of the sleep epoch in \mathfrak{R}^{2m_1} , where m_1 are the hidden units of the GRU layer. In (4) they exploit the positional embedding approach recently proposed in [36] to include the whole night PSG context of each epoch in the following

sequence encoder block. First, they build a vector $v = [i_t^{epoch}, i_{t,30}^{cycle}, \dots, i_{t,150}^{cycle}] \in \mathfrak{R}^6$ for each epoch, where $i_t^{epoch} = \frac{t}{1200}$ is the epoch index and $i_{t,l}^{cycle} = \cos\left(\frac{t\pi}{l}\right)$ with l in [30, 60, 90, 120, 150] are the cyclic indexes. The vector v is then projected using the Linear+Relu layer to output the positional embedding i_t of each epoch. Finally, i_t is concatenated with the output of the attention layer to obtain the epoch representation $a_t \in \mathfrak{R}^{2m_1+6}$.

The *sequence encoder* part, or what we refer to as sequence processing block (*SPB*), is designed to process sequences of epochs, and it aims to encode the temporal information (e.g. stage transition rules). The *SPB* block consists of two layers of bidirectional gated recurrent unit (GRU) with skip-connections (SkipGRU) and the softmax classification layer. The sequence of epochs a_1, \dots, a_t is fed to the *SPB* block to output for each epoch the sleep stage probabilities $\hat{p}_k \in \mathfrak{R}^5$. The softmax function, together with the cross-entropy loss function H , is used to train the model to output the probabilities \hat{p}_k for the five mutually exclusive classes K that correspond to the five sleep stages.

DSN-L and SSN are trained end-to-end via backpropagation aiming to minimize the above mentioned cross-entropy loss function (8). The models are trained using mini-batch Adam gradient-based optimizer [37] with a learning rate lr . The training procedure runs up to a maximum number of iterations (e.g. 100 iterations), as long as the break early stopping condition is satisfied (i.e. the validation F1-score stopped improving after more than a certain epochs; the model with the best validation F1-score is used at test time). All the training parameters (e.g. adam-optimizer parameters beta1 and beta2, mini-batch size, learning rate etc.) are all set as recommended in [32] and [23].

Label smoothing with *Soft-Consensus*

The predicted sleep stage for each 30-second epoch $x(t)$ is associated to a probability value \hat{p}_i , which should mirror its ground truth correctness likelihood. When this happens, we can state that the model is well calibrated, or that the model provides a *calibrated confidence* measure along with its prediction [38]. Consider, for example, a model trained to classify images as either containing a dog or not; out of ten test set images it outputs the probability of there being a dog as 0.60 for every image. The model is perfectly calibrated if six dog images are present in the test set. Label smoothing [39] has been shown to be a suitable technique to improve the calibration of the model.

By default, the cross-entropy loss function is computed between the prediction \hat{p}_i and the target \bar{y}_i (i.e. the one-hot encoded sleep stages, 1 for the correct class and 0 for all the other classes). When the model is trained with the label smoothing technique, the hard target is smoothed with the standard *uniform* distribution $1/K$ (9). Thus, the cross-entropy loss function (10) is minimized by using the weighted mixture of the target $y_{i,k}^{LS_u}$.

$$y_{i,k}^{LS_u} = y_{i,k} \cdot (1 - \alpha) + \alpha \cdot 1/K \quad (9)$$

$$H(\bar{y}_i, \hat{p}_i) = \sum_{k=1}^K -y_{i,k}^{LS_u} \cdot \log(\hat{p}_{i,k}) \quad (10)$$

where α is the smoothing parameter, K the number of sleep stages, $y_{i,k}^{LS_u}$ the weighted mixture of the target and $\hat{p}_{i,k}$ the output of the softmax layer with the predicted probability values.

In our study, we exploit the label smoothing technique to improve the insertion of the knowledge from the multiple-scorers in the learning process. We propose to use the *Soft-Consensus* (11) as our new distribution to smooth the hard target $y_{i,k}$.

$$Soft-Consensus_i = \frac{\#(Y_i = y_{i,k})}{M} \quad (11)$$

where Y_i is the set of observations - i.e. annotations given by the different physicians - for the i -th epoch, k is the class index, M is the number of observations and $\#$ is the cardinality of the set $(Y_i = y_{i,k})$. In simple words, the probability value for each sleep stage k is computed as the sum of its occurrences divided by the total number of observations.

$Soft-Consensus_{i,k} \in [0, 1]^{1 \times K}$ is the one-dimensional vector that we use to smooth the hard target (12), and then minimize the cross-entropy loss function (13).

$$y_{i,k}^{LS_{sc}} = y_{i,k} \cdot (1 - \alpha) + \alpha \cdot Soft-Consensus_{i,k} \quad (12)$$

$$H(\bar{y}_i, \bar{p}_i) = \sum_{k=1}^K - y_{i,k}^{LS_{sc}} \cdot \log(\hat{p}_{i,k}) \quad (13)$$

As an example, consider the following set of observations $Y_i = [W, W, W, N1, N2]$ given by five different physicians for the same i -th epoch.

By applying (11) and (12) we obtain the following $y_{i,k}^{LS_{sc}}$ smoothed hard-target:

$$Soft-Consensus_{i,k} = [p_W = 3/5, p_{N1} = 1/5, p_{N2} = 1/5, p_{N3} = 0/5, p_{REM} = 0/5]$$

$$Soft-Consensus_{i,k} = [0.6, 0.2, 0.2, 0, 0]$$

$$y_{i,k}^{LS_{sc}} = y_{i,k} \cdot (1 - \alpha) + \alpha \cdot \text{Soft-Consensus}_{i,k} = [0.8, 0.1, 0.1, 0, 0]$$

with the one-hot encoded target $y_{i,k} = [p_W = 1, p_{N1} = 0, p_{N2} = 0, p_{N3} = 0, p_{REM} = 0]$

and $\alpha = 0.5$.

We perform a simple grid-search to set the smoothing hyperparameter α . When the model is trained with the labels smoothed by the *uniform* distribution the α value ranges between $(0, 0.5]$ with step 0.1. Extreme values are not considered as for $\alpha = 0$ the model is trained using the standard hot-encoding vector; whilst for values higher than 0.5, e.g. $\alpha = 1$, the model would be trained using mainly/only the uniform distribution $1/K$ for each sleep stage. When the model is trained with the labels smoothed by the *Soft-Consensus* distribution the α value ranges between $(0, 1]$ with step 0.1. In the latter case we also investigate an α value equal to 1 to evaluate the full impact of the consensus distribution on the learning procedure.

Monte Carlo dropout and query procedure

In [32] we proposed to exploit the Monte Carlo (MC) dropout technique [43] to further enhance the performance of a sleep scoring architecture. By definition, the *dropout* layer shuts down, randomly at each iteration, a certain number of units of our network during the training phase. It randomly samples a certain number of sub-networks at each iteration. The *dropout* layer, by default, is active only during the training phase, whilst at test time all the trained neurons and connections are used, *i.e.*, all the weights of the network. By applying the *dropout* M times even at test time, we sample M different sub-networks from the space of all the possible models, and we end up with M different predictions. Thus, we can compute

the *mean* $\mu_{i,k} = \frac{\sum_{m=1}^M \hat{p}_{m,i,k}}{M}$ of the M predictions for each sleep stage k , where $\hat{p}_{m,i,k}$ is the

output probability value for the sleep stage k of the m -th prediction for the i -th 30-second epoch. The $\mu_{i,k}$ outputs could be interpreted as an averaging ensemble of all the sampled

sub-networks. The final prediction $\hat{y}_{i,MC}$ of the ensembling models will be given by

$\hat{y}_{i,MC} = \text{argmax}(\mu_i)$. We exploit the *MC* dropout technique to evaluate the increase in performance on both the architectures DSN-L and SSN on all the experimented databases. In [32] we also introduced a query procedure to estimate the uncertain predictions given by the model. The query procedure simply relies on the setting of a fixed threshold value $q\% = 5\%$, that corresponds to a percentage of sleep epochs to select/reject and to send potentially to the physician for a secondary review. The epochs with the lowest probability values are the $q\%$ selected (on average up to 50 epochs for each PSG recording). In this study we simply use the predicted probability values $\hat{y}_i = \text{argmax}(\hat{p}_{i,k})$ to select/reject the uncertain sleep epochs.

Experimental design

We evaluate DeepSleepNet-Lite (DSN-L) and SimpleSleepNet (SSN) using the k -fold cross-validation scheme. We set k equal to 10 for IS-RC, 25 for DOD-H (leave-one-out evaluation procedure) and 10 for DOD-O datasets, consistent with what was done in [23]. In Table 2 we summarize the data split for each dataset.

The following experiments are conducted on both DSN-L and SSN models for each dataset:

- **base**. The models are trained without label smoothing.
- **base+LS_U**. The models are trained with label smoothing using the standard *1/K uniform* distribution - i.e. the hard targets (scorer consensus) are weighted with the *uniform* distribution.
- **base+LS_{sc}**. The models are trained with label smoothing using the proposed *Soft-Consensus* - i.e. the hard targets (scorer consensus) are weighted with the *Soft – Consensus* distribution.

These models, differently trained, have been evaluated with and without *MC* dropout ensemble technique. In Table 4, 5 and 6 subsection **Analysis of experiments** we present

the results obtained for each experiment on both DSN-L and SSN evaluated on IS-RC, DOD-H and DOD-O datasets.

Metrics

Performance.

The per-class F1-score, the overall accuracy (Acc.), the macro-averaging F1-score, the weighted-averaging F1-score (i.e. the metric is weighted by the number of true instances for each label, so as to consider the high imbalance between the sleep stages) and the Cohen's kappa have been computed per-subject from the predicted sleep stages from all the folds to evaluate the performance of our model [40, 41].

Hypnodensity graph.

The hypnodensity-graph is an efficient visualization tool introduced in [27] to plot the probability distribution over each sleep stage for each 30-second epoch over the whole night. Unlike the standard hypnogram sleep cycle visualization tool, it shows the probability of occurrence of each sleep stage for each 30-second epoch; so it is not limited to the discrete sleep stage value (see Figure 3). In our study we have used the hypnodensity-graph to display both the model output - i.e. the *softmax* output probability vectors $\hat{p}_{i,k}$ - and the multi-scorer *Soft-Consensus*_{*i,k*} probability distributions.

The Averaged Cosine Similarity (*ACS*) is used to quantify the similarity between the hypnodensity-graph generated by the model and the hypnodensity-graph generated by the *Soft-Consensus*. The *ACS* has been computed as follows:

$$ACS = \frac{1}{N} \sum_{i=1}^N \frac{Soft-Consensus_{i,k} \cdot \hat{p}_{i,k}}{\|Soft-Consensus_{i,k}\| \cdot \|\hat{p}_{i,k}\|} \quad (14)$$

where N is the number of epochs in the whole night, $\|\cdot\|$ is the norm computed for the predicted probability vector $\hat{p}_{i,k}$ and the *Soft-Consensus* _{i,k} ground-truth vector for the i -th epoch. Thus, the cosine-similarity is averaged across all the epochs N to obtain our averaged *ACS* unique score of similarity. The cosine-similarity values may range between 0 i.e. high dissimilarity and 1 i.e. high similarity between the vectors.

Calibration.

The calibration of the model is evaluated by using the expected calibration error (*ECE*) metric proposed in [42]. By (*ECE*) we compute the difference in expectation between the accuracy acc and the $conf$ (i.e. the *softmax* output probabilities) values. More in detail, the predictions are divided into M equally spaced bins (with size $1/M$), then we compute the accuracy $acc(B_m)$ and the average predicted probability value $conf(B_m)$ for each bin as follows:

$$acc(B_m) = \frac{1}{|B_m|} \cdot \sum_{i \in B_m} 1(\hat{y}_i = y_i) \quad (15)$$

$$conf(B_m) = \frac{1}{|B_m|} \cdot \sum_{i \in B_m} \hat{p}_i \quad (16)$$

where y_i is the true label and $\hat{y}_i = \operatorname{argmax}(\hat{p}_{i,k})$ is the predicted label for the i -th epoch;

B_m is the group of samples whose predicted probability values fall in $I_m = (\frac{m-1}{M}, \frac{m}{M}]$ and

$\hat{p}_i = \max(\hat{p}_{i,k})$ is the predicted probability value for sample the i -th 30-second epoch.

Finally, the *ECE* value is computed as the weighted average of the difference between the acc and the $conf$ among the M bins:

$$ECE = \sum_{m=1}^M \frac{|B_m|}{n_B} \cdot |acc(B_m) - conf(B_m)| \quad (17)$$

where n_B is the number of samples in each bin. Perfectly calibrated models have

$acc(B_m) = conf(B_m)$ for all $m \in \{1, \dots, M\}$, resulting in $ECE = 0$.

Results

Analysis of experiments

In [Table 3](#) we first report for all the multi-scored databases IS-RC, DOD-H and DOD-O, the overall scorers performance and their *Soft – Agreement (SA)*, i.e. the agreement of each scorer with the consensus among the physicians. On IS-RC we have on average a lower inter-scorer agreement (*SA* equal to 0.69, with an F1-score 69.7%) compared to both DOD-H and DOD-O (*SA* equal to 0.89 and 0.88, with an F1-score 88.1% and 86.4% respectively). Consequently, we expect a higher efficiency of our label smoothing with the *Soft – Consensus* approach (*base+LS_{SC}*) on the experiments conducted on the IS-RC database. The lower the inter-scorer agreement, the lower should be the performance of a model trained with the one-hot encoded labels (i.e. the majority vote weighted by the degree of consensus from each physician).

In [Table 4](#) and [Table 5](#) we report the overall performance, the calibration measure and the hypnodensity similarity measure of the three different DSN-L and SSN models on the three databases IS-RC, DOD-H and DOD-O. The performance of the DSN-L *base* models are higher compared to the performance averaged among the scorers on the IS-RC database, but not on the DOD-H and DOD-O databases. In contrast, the performance of the SSN *base* models are always higher than the performance averaged among the scorers on all the databases. We highlight that the results we report for SSN on DOD-H and DOD-O are slightly different compared to the one reported in [\[23\]](#). We decided to not compute a weight (from 0 to 1) for each epoch, based on how many scorers voted for the consensus. We do not balance the importance of each epoch when we compute the above mentioned metrics.

We think it is unfair to constrain any metrics based on the amount of voting physicians. Overall, the results show an improvement in performance (i.e overall accuracy, MF1-score, Cohen's kappa (k), and F1-score) from the *base* models to the ones trained with label smoothing along with the proposed *Soft – Consensus* distribution (i.e. *base+LS_{SC}*) on all the databases. The *ACS* is the metric that best quantifies the ability of the model in adapting to the consensus of the group of scorers. A higher *ACS* value means a higher similarity between the hypnodensity-graph generated by the model and the hypnodensity-graph generated by the *Soft – Consensus* (i.e. the model better adapts to the consensus of the group of physicians). As all the other metrics the *ACS* value is computed per subject, we report the mean and also the standard deviation across subjects ($\mu \pm \sigma$). We found a significant improvement in the *ACS* value from the *base* models to the *base+LS_{SC}* models on all the databases on DSN-L (p-values < 0.01) and on SSN (p-values < 0.05). Hence, our approach enables both the DSN-L and the SSN architectures to significantly adapt to the consensus of the group of physicians on all the multi-scored datasets.

We could easily infer that the SSN architecture is better (i.e. higher performance) compared to our DSN-L architecture. The purpose of our study is not to highlight whether one architecture is better than the other, but we can not fail to notice the high values of confidence (the *conf* value is the average of the softmax output max-probabilities) obtained on the SSN based models. High values of confidence still persist despite smoothing the labels (with both *uniform* and *Soft-Consensus* distributions) during the training procedure. The SSN architecture is not highly responsive to the changes in probability values we implemented on the one-hot encoded labels. It always rely/overfit on the *max* probability value given for each epoch, i.e. the consensus among the five/six different scorers. Indeed, on the IS-RC, which is the database with the lower inter-scorer agreement, the SSN *base+LS_{SC}* model reaches a higher value of F1-score, i.e. 81.6%, compared to our DSN-L *base+LS_{SC}* model, i.e. 75.9% , but a lower value of *ACS* (0.817 on SSN and 0.836 on DSN-L, with a p-value < 0.01). The SSN model overfit to the majority vote or the *max* probability

value given for each epoch, whilst the DSN-L better adapts to the consensus of the group of scorers (i.e better encode the variability among the physicians).

The last statement is also strengthened by the Supplementary [Figure S1](#) and [Figure S2](#). For DSN-L and SSN we report the *ACS* values across all the experimented α values, on both the *base+LS_U* and the *base+LS_{SC}* models tested on the three databases. As expected, the DSN-L model shows a high sensitivity in ACS values to changes in α -hyperparameter across all databases. This sensitivity is not as strong with the SSN model. Clearly, we do not achieve the same results on the experiments performed on the *base+LS_U*. Unlike the *Soft-Consensus* distribution, the *uniform* distribution is not equally suitable to represent the complexity of the degree of agreement between the different physicians.

In our study we also exploit the Monte Carlo dropout ensembling technique to further enhance the performance of the models. We apply *MC* dropout $M = 30$ times at inference time. In [Table 6](#) we show that, overall, on all the experiments, we obtained a slight improvement (up to 4%) on our best *base+LS_{SC}* models, on IS-RC, DOD-H and DOD-O datasets.

Query procedure

In Supplementary [Table S1](#) we report the overall performance achieved on the DeepSleepNet-Lite models on IS-RC, DOD-H and DOD-O datasets as a result of the query procedure. Specifically, the metrics refer to the epochs kept after the $\text{argmax}(\hat{p}_{i,k})$ selection procedures ($q\%$ threshold value fixed to 5%). We also quantify the percentage of misclassified epochs (%miscl.) among the rejected after the query procedure. The percentage of misclassified epochs is on average in the range 50% to 60%. Consequently, on all the models we have an increase in performance up to 2%-3% in F1-score. These results highlight the efficiency of the query procedure to select a good enough number of misclassified epochs among the selected one.

Unlike what we expected, it is not always the case that a better calibrated architecture leads to a better estimate of the model uncertainty. A lower *ECE* value (see [Table 4](#)) does not always enable the detection of a significantly higher number of percentages of misclassified epochs (%miscl.).

Discussion

In this work, we demonstrate the efficiency of label smoothing along with the *Soft – Consensus* distribution in encoding the scorers’s variability into the training procedure of both DeepSleepNet-Lite and SimpleSleepNet scoring algorithms. The results show an improvement in overall performance from the *base* models to the ones trained with *base+LS_{SC}*. We introduce the averaged cosine similarity metric to better quantify the similarity between the probability distribution predicted by the models and the ones generated by the scorer consensus. We obtained a significant improvement in the *ACS* values from the *base* models to the *base+LS_{SC}* models on both DeepSleepNet-Lite and SimpleSleepNet architectures. Based on the reported high confidence values, we found that SimpleSleepNet tends to overfit on each dataset. Specifically, it tends to overfit on the majority vote weighted by the degree of consensus from each physician, but does not encode as well their variability. In this study we aim at highlighting a simple procedure exploitable to train a standard deep learning based model with multiple supervised signals. The procedure enables us to transfer the variability, the uncertainty, and the noise we have by nature on the labels into the models. Our approach results quite effective in encoding the complexity of the scorers’ consensus within the classification algorithm, whose importance is often underestimated. Moreover, by leveraging both the *LS_{SC}* technique and the uncertainty estimate procedure described above, we are able to increase the percentage of detected misclassified epochs among those discarded/removed (up to 60%).

In summary, the possibility of exploiting the full set of information that is hidden in a multi-scored dataset would certainly enhance automated deep learning algorithms performance. However, in order to generalize our approach, there are two big limitations. The first is that a far bigger datasets, highly heterogeneous (with different diagnosis, age range, gender etc.) scored by multiple physicians would be necessary. The second is that to transfer consensus variability from a dataset to another would require finding a relation between the consensus variability and a complex, not easy to define, deep learning characteristic related to the epoch itself. The present approach enables us to better adapt to the consensus of the group of scorers, and, as a consequence, to better quantify the uncertainty and the disagreement we have between the different scorers.

Supplementary material

Supplementary material is available at arxiv online.

Funding

Prof. F. D. Faraci was supported by SPAS: Sleep Physician Assistant System project, from Eurostars funding programme. Prof. P. Favaro was supported by the IRC Decoding Sleep: From Neurons to Health and Mind, from the University of Bern, Switzerland.

Disclosure Statement

Conflicts of interest. The authors declare that they have no conflict of interest.

References

- [1] National Center on Sleep Disorders Research, National Inst. Health Sleep Disorders Res. Plan, Bethesda, MD, USA, 2011.
- [2] C. Iber, S. Ancoli-Israel, A. L. Chesson, and S. F. Quan, *The AASM Manual for the Scoring of Sleep and Associated Events: Rules, Terminology, and Technical Specifications*. Westchester, IL, USA: American Academy Sleep Medicine, 2007.
- [3] Rosenberg RS, Van Hout S. The American academy of sleep medicine inter-scorer reliability program: sleep stage scoring. *J Clin Sleep Med* 2013;9(01):81e7.
- [4] Younes M, Raneri J, Hanly P. Staging sleep in polysomnograms: analysis of inter-scorer variability. *J Clin Sleep Med* 2016;12(06):885e94.
- [5] Muto V, Berthomier C, Schmidt C, Vandewalle G, Jaspar M, Devillers J, et al. 0315 Inter-and intra-expert variability in sleep scoring: comparison between visual and automatic analysis. *Sleep* 2018;41(suppl_1):A121.
- [6] Danker-hopfe H, Anderer P, Zeitlhofer J, Boeck M, Dorn H, Gruber G, et al. Interrater reliability for sleep scoring according to the Rechtschaffen & Kales and the new AASM standard. *J Sleep Res* 2009;18(1):74e84.
- [7] Aboalayon K, Faezipour M, Almuhammadi W, Moslehpour S. Sleep stage classification using EEG signal analysis: a comprehensive survey and new investigation. *Entropy* 2016;18(9):272.
- [8] Ronzhina M, Janoušek O, Kolářová J, Nováková M, Honzík P, Provazník I. Sleep scoring using artificial neural networks. *Sleep medicine reviews*. 2012 Jun 1;16(3):251-63.
- [9] L. Fiorillo et al., "Automated sleep scoring: A review of the latest approaches," *Sleep Medicine Reviews*, vol. 48, pp. 101204, 2019.
- [10] O. Faust et al., "A review of automated sleep stage scoring based on physiological signals for the new millennia," *Comput Methods Programs Biomed*, vol. 176, pp. 81–91, 2019.

- [11] Tsinalis, Orestis, Paul M. Matthews, and Yike Guo. "Automatic sleep stage scoring using time-frequency analysis and stacked sparse autoencoders." *Annals of biomedical engineering* 44.5 (2016): 1587-1597.
- [12] Dong, Hao, et al. "Mixed neural network approach for temporal sleep stage classification." *IEEE Transactions on Neural Systems and Rehabilitation Engineering* 26.2 (2017): 324-333.
- [13] Vilamala, Albert, Kristoffer H. Madsen, and Lars K. Hansen. "Deep convolutional neural networks for interpretable analysis of EEG sleep stage scoring." 2017 IEEE 27th International Workshop on Machine Learning for Signal Processing (MLSP). IEEE, 2017.
- [14] Chambon, Stanislas, et al. "A deep learning architecture for temporal sleep stage classification using multivariate and multimodal time series." *IEEE Transactions on Neural Systems and Rehabilitation Engineering* 26.4 (2018): 758-769.
- [15] Cui, Zhihong, et al. "Automatic Sleep Stage Classification Based on Convolutional Neural Network and Fine-Grained Segments." *Complexity* 2018 (2018).
- [16] Patanaik, Amiya, et al. "An end-to-end framework for real-time automatic sleep stage classification." *Sleep* 41.5 (2018): zsy041.
- [17] Sors, Arnaud, et al. "A convolutional neural network for sleep stage scoring from raw single-channel EEG." *Biomedical Signal Processing and Control* 42 (2018): 107-114.
- [18] Yildirim, Ozal, Ulas Baran Baloglu, and U. Rajendra Acharya. "A deep learning model for automated sleep stages classification using psg signals." *International journal of environmental research and public health* 16.4 (2019): 599
- [19] Olesen AN, Jørgen Jennum P, Mignot E, Sorensen HB. Automatic sleep stage classification with deep residual networks in a mixed-cohort setting. *Sleep*. 2021 Jan;44(1):zsaa161.
- [20] Perslev M, Darkner S, Kempfner L, Nikolic M, Jennum PJ, Igel C. U-Sleep: resilient high-frequency sleep staging. *NPJ digital medicine*. 2021 Apr 15;4(1):1-2.

[21] Michielli, Nicola, U. Rajendra Acharya, and Filippo Molinari. "Cascaded LSTM recurrent neural network for automated sleep stage classification using single-channel EEG signals." *Computers in biology and medicine* 106 (2019): 71-81.

[22] H. Phan, F. Andreotti, N. Cooray, O. Y. Chén, and M. De Vos, "SeqSleepNet: end-to-end hierarchical recurrent neural network for sequence-to-sequence automatic sleep staging," *IEEE Trans. on Neural Systems and Rehabilitation Engineering (TNSRE)*, vol. 27, no. 3, pp. 400–410, 2019.

[23] A. Guillot, F. Sauvet, E. H. During, and V. Thorey, "Dreem open datasets: Multi-scored sleep datasets to compare human and automated sleep staging," *IEEE Transactions on Neural Systems and Rehabilitation Engineering*, vol. 28, no. 9, pp. 1955–1965, 2020.

[24] Supratak, Akara, et al. "DeepSleepNet: A model for automatic sleep stage scoring based on raw single-channel EEG." *IEEE Transactions on Neural Systems and Rehabilitation Engineering* 25.11 (2017): 1998-2008.

[25] Biswal, Siddharth, et al. "Expert-level sleep scoring with deep neural networks." *Journal of the American Medical Informatics Association* 25.12 (2018): 1643-1650.

[26] Malafeev, Alexander, et al. "Automatic human sleep stage scoring using deep neural networks." *Frontiers in neuroscience* 12 (2018): 781.

[27] Stephansen, Jens B., et al. Neural network analysis of sleep stages enables efficient diagnosis of narcolepsy. *Nature communications*, 2018, 9.1: 1-15.

[28] Mousavi, Sajad; AFGHAH, Fatemeh; ACHARYA, U. Rajendra. SleepEEGNet: Automated sleep stage scoring with sequence to sequence deep learning approach. *PloS one*, 2019, 14.5: e0216456.

[29] Phan, Huy, et al. XSleepNet: Multi-view sequential model for automatic sleep staging. *IEEE Transactions on Pattern Analysis and Machine Intelligence*, 2021.

U-Sleep

[30] Maurice Abou Jaoude, Haoqi Sun, Kyle R Pellerin, Milena Pavlova, Rani A Sarkis, Sydney S Cash, M Brandon Westover, Alice D Lam, Expert-level automated sleep staging of

long-term scalp electroencephalography recordings using deep learning, *Sleep*, Volume 43, Issue 11, November 2020, zsaa112, <https://doi.org/10.1093/sleep/zsaa112>

[31] Kuna ST, Benca R, Kushida CA, Walsh J, Younes M, Staley B, Hanlon A, Pack AI, Pien GW, Malhotra A. Agreement in computer-assisted manual scoring of polysomnograms across sleep centers. *Sleep*. 2013 Apr 1;36(4):583-9.

[32] Fiorillo L, Favaro P, Faraci FD. Deepsleepnet-lite: A simplified automatic sleep stage scoring model with uncertainty estimates. *IEEE Transactions on Neural Systems and Rehabilitation Engineering*. 2021 Oct 14;29:2076-85.

[33] Cohen, Mike X. *Analyzing neural time series data: theory and practice*. MIT press, 2014.

[34] Ioffe S, Szegedy C. Batch normalization: Accelerating deep network training by reducing internal covariate shift. In *International conference on machine learning 2015 Jun 1* (pp. 448-456). PMLR.

[35] Luong MT, Pham H, Manning CD. Effective approaches to attention-based neural machine translation. *arXiv preprint arXiv:1508.04025*. 2015 Aug 17.

[36] Vaswani A, Shazeer N, Parmar N, Uszkoreit J, Jones L, Gomez AN, Kaiser Ł, Polosukhin I. Attention is all you need. *Advances in neural information processing systems*. 2017;30.

[37] Kingma DP, Ba J. Adam: A method for stochastic optimization. *arXiv preprint arXiv:1412.6980*. 2014 Dec 22.

[38] Guo C, Pleiss G, Sun Y, Weinberger KQ. On calibration of modern neural networks. In *International Conference on Machine Learning 2017 Jul 17* (pp. 1321-1330). PMLR.

[39] Szegedy C, Vanhoucke V, Ioffe S, Shlens J, Wojna Z. Rethinking the inception architecture for computer vision. In *Proceedings of the IEEE conference on computer vision and pattern recognition 2016* (pp. 2818-2826).

[40] Cohen, Jacob. A coefficient of agreement for nominal scales. *Educational and psychological measurement*, 1960, 20.1: 37-46.

[41] Sokolova, Marina; Lapalme, Guy. A systematic analysis of performance measures for classification tasks. *Information processing & management*, 2009, 45.4: 427-437.

[42] Naeini, Mahdi Pakdaman; Cooper, Gregory F.; Hauskrecht, Milos. Obtaining well calibrated probabilities using bayesian binning. AAAI Conference on Artificial Intelligence. AAAI Conference on Artificial Intelligence. NIH Public Access, 2015. p. 2901.

[43] Gal, Yarin; Ghahramani, Zoubin. Dropout as a bayesian approximation: Representing model uncertainty in deep learning. In: international conference on machine learning. 2016. p. 1050-1059.

Tables

Table 1

Number and percentage of 30-second epochs per sleep stage for the IS-RC, DOD-H and DOD-O datasets.

	W	N1	N2	N3	R	Total
IS-RC	24517 (29.1%)	3773 (4.5%)	40867 (48.5%)	3699 (4.4%)	11475 (13.6%)	84331
DOD-H	3075 (12.5%)	1463 (5.9%)	12000 (48.7%)	3442 (14.0%)	4685 (19.0%)	24665
DOD-O	10520 (19.8%)	2739 (5.1%)	26213 (49.2%)	5617 (10.6%)	8147 (15.3%)	53236

Table 2

Data split on the IS-RC, DOD-H and DOD-O datasets.

	Size	Experimental Setup	Held-out Validation Set	Held-out Test Set
IS-RC	70	10-fold CV	13 subjects	7 subject
DOD-H	25	25-fold CV	6 subjects	1 subjects
DOD-O	55	10-fold CV	12 subjects	6 subjects

Table 3

Scorers performance on IS-RC, DOD-H and DOD-O dataset with *Soft – Agreement (SA)*, overall accuracy (%Acc.), macro F1-score (%MF1), Cohen’s Kappa (*k*), weighted-averaging F1-score (%F1) and % per-class F1-score. The scorer with the best performance (i.e. high agreement with the consensus among the six different physicians) is indicated in bold.

			Overall Metrics				Per-Class F1-Score				
	Scorers	SA	Acc.	MF1	<i>k</i>	F1	W	N1	N2	N3	R
IS-RC	Scorer-1	0.79	83.0	69.5	0.72	83.8	83.1	47.2	87.3	48.0	82.1
	Scorer-2	0.81	89.4	72.8	0.82	89.2	91.3	57.6	92.5	32.9	89.8
	Scorer-3	0.53	40.7	26.5	0.11	40.8	29.8	14.7	54.5	17.9	15.6
	Scorer-4	0.52	38.9	26.1	0.12	40.5	28.6	14.7	54.2	15.4	17.5
	Scorer-5	0.70	73.7	61.6	0.63	75.8	88.7	36.9	70.2	25.8	86.2
	Scorer-6	0.79	87.2	77.2	0.81	88.2	92.5	54.6	89.4	59.8	89.5
	Average	0.69	68.7	55.5	0.53	69.7	68.9	37.6	74.7	33.3	63.5
DOD-H	Scorer-1	0.88	87.0	81.5	0.81	87.4	87.5	60.0	89.4	84.8	85.7
	Scorer-2	0.91	89.3	84.1	0.84	89.7	87.4	65.1	91.6	84.3	92.2
	Scorer-3	0.92	90.6	84.5	0.86	90.4	89.9	67.5	92.1	77.9	95.3
	Scorer-4	0.84	82.6	76.7	0.75	83.1	76.5	49.1	85.4	80.7	92.0
	Scorer-5	0.92	89.9	83.6	0.85	89.9	86.7	66.0	92.1	81.0	92.2
	Average	0.89	87.9	82.1	0.82	88.1	85.5	61.5	90.0	81.7	91.5
DOD-O	Scorer-1	0.87	85.0	75.1	0.77	84.6	90.0	49.5	85.2	67.6	83.3
	Scorer-2	0.87	85.0	78.2	0.78	86.0	89.3	58.4	85.4	69.1	88.6
	Scorer-3	0.88	86.0	75.0	0.78	84.6	91.0	54.3	86.5	56.1	87.0
	Scorer-4	0.88	86.7	77.7	0.80	87.2	91.2	59.3	89.4	62.9	85.8
	Scorer-5	0.91	89.9	82.3	0.84	90.0	93.7	68.3	90.7	70.5	88.2
	Average	0.88	86.5	77.6	0.79	86.4	91.0	58.0	87.3	65.2	86.5

Table 4

Overall metrics, per-class F1-score, calibration and ACS hypnodensity graph similarity measures of the DeepSleepNet-Lite models obtained from 10-fold cross-validation on IS-RC dataset, from 25-fold cross-validation on DOD-H dataset, and from 10-fold cross-validation on DOD-O dataset. Best shown in bold.

			Overall Metrics				Per-Class F1-Score					Calibration		Hypn.
	Models	α	Acc.	MF1	k	F1	W	N1	N2	N3	R	ECE	<i>conf.</i>	ACS
IS-RC	<i>base</i>	-	69.6	50.6	0.56	70.0	81.6	11.8	71.9	27.2	60.7	0.096	79.0	0.772 \pm 0.075
	<i>base+LS_U</i>	0.4	74.8	57.0	0.63	75.8	83.3	24.3	79.0	30.6	67.7	0.296	45.2	0.806 \pm 0.042
	<i>base+LS_{SC}</i>	0.6	75.8	56.5	0.69	75.9	83.5	19.5	79.7	33.3	66.4	0.190	56.7	0.836 \pm 0.041
DOD-H	<i>base</i>	-	76.9	70.0	0.68	77.2	79.7	39.5	78.8	76.5	75.2	0.163	92.7	0.817 \pm 0.097
	<i>base+LS_U</i>	0.2	75.3	68.7	0.66	75.2	78.8	40.0	75.9	72.0	76.8	0.059	68.9	0.829 \pm 0.068
	<i>base+LS_{SC}</i>	0.8	80.2	72.4	0.72	80.4	80.4	42.3	83.4	77.6	78.8	0.016	81.4	0.873 \pm 0.053
DOD-O	<i>base</i>	-	77.3	67.8	0.66	78.0	80.7	41.2	81.0	68.1	68.3	0.131	90.2	0.840 \pm 0.073
	<i>base+LS_U</i>	0.1	77.5	68.0	0.67	78.2	80.8	41.9	80.4	68.4	68.7	0.009	78.4	0.859 \pm 0.072
	<i>base+LS_{SC}</i>	1	79.4	69.6	0.69	79.9	80.4	43.8	83.5	72.5	68.1	0.009	78.3	0.878 \pm 0.061

Table 5

Overall metrics, per-class F1-score, calibration and ACS hypnodensity graph similarity measures of the SimpleSleepNet models obtained from 10-fold cross-validation on IS-RC dataset, from 25-fold cross-validation on DOD-H dataset, and from 10-fold cross-validation on DOD-O dataset. Best shown in bold.

			Overall Metrics				Per-Class F1-Score					Calibration		Hypn.
	Models	α	Acc.	MF1	k	F1	W	N1	N2	N3	R	ECE	<i>conf.</i>	ACS
IS-RC	<i>base</i>	-	81.8	60.8	0.72	80.8	86.3	29.9	85.3	24.3	78.1	0.174	99.4	0.806 \pm 0.052
	<i>base+LS_U</i>	0.3	82.5	59.8	0.72	81.1	86.5	28.8	86.5	18.7	78.7	0.169	99.3	0.811 \pm 0.058
	<i>base+LS_{SC}</i>	0.7	83.1	60.2	0.73	81.6	86.7	27.6	86.8	20.1	79.8	0.162	99.2	0.817 \pm 0.047
DOD-H	<i>base</i>	-	87.1	80.2	0.81	87.1	83.6	55.5	90.0	83.3	89.0	0.126	99.7	0.890 \pm 0.047
	<i>base+LS_U</i>	0.4	87.6	81.0	0.81	87.5	85.5	57.3	90.2	82.1	90.3	0.120	99.5	0.899 \pm 0.034
	<i>base+LS_{SC}</i>	0.5	88.8	82.3	0.83	88.7	86.4	58.8	90.9	83.2	92.1	0.108	99.6	0.907 \pm 0.039
DOD-O	<i>base</i>	-	85.3	75.9	0.77	85.2	88.2	50.4	87.1	65.9	88.0	0.145	99.7	0.889 \pm 0.056
	<i>base+LS_U</i>	0.1	85.6	75.8	0.78	85.2	88.2	51.2	87.3	64.3	88.4	0.141	99.6	0.893 \pm 0.052
	<i>base+LS_{SC}</i>	1	86.8	77.7	0.79	86.7	89.0	51.0	88.3	69.3	91.1	0.125	99.2	0.906 \pm 0.043

Table 6

Overall metrics and *ACS* hypnodensity graph similarity measures on the DeepSleepNet-Lite and SimpleSleepNet *base+LS_{SC}* models, obtained from 10-fold cross-validation on IS-RC dataset, from 25-fold cross-validation on DOD-H dataset, and from 10-fold cross-validation on DOD-O dataset with and without *MC*. Best shown in bold.

			Overall Metrics				Hypn.
			Acc.	MF1	<i>k</i>	F1	<i>ACS</i>
IS-RC	DSN-L	w/o MC	75.8	56.5	0.69	75.9	0.836 ± 0.041
		w/ MC	78.6	57.6	0.67	78.0	0.850 ± 0.036
	SSN	w/o MC	83.1	60.2	0.73	81.6	0.817 ± 0.047
		w/ MC	83.0	59.2	0.73	81.1	0.818 ± 0.048
DOD-H	DSN-L	w/o MC	80.2	72.4	0.72	80.4	0.873 ± 0.053
		w/ MC	84.4	75.9	0.76	84.2	0.906 ± 0.026
	SSN	w/o MC	88.8	82.3	0.83	88.7	0.907 ± 0.039
		w/ MC	89.1	82.6	0.84	89.0	0.910 ± 0.039
DOD-O	DSN-L	w/o MC	79.4	69.6	0.69	79.9	0.878 ± 0.061
		w/ MC	80.7	70.8	0.71	80.9	0.889 ± 0.059
	SSN	w/o MC	86.8	77.7	0.79	86.7	0.906 ± 0.043
		w/ MC	87.1	78.0	0.80	86.9	0.909 ± 0.041

Figure Captions

Figure 1. DeepSleepNet-Lite architecture.

An overview of the *representation learning* architecture from [24], with our *sequence-to-epoch* training approach.

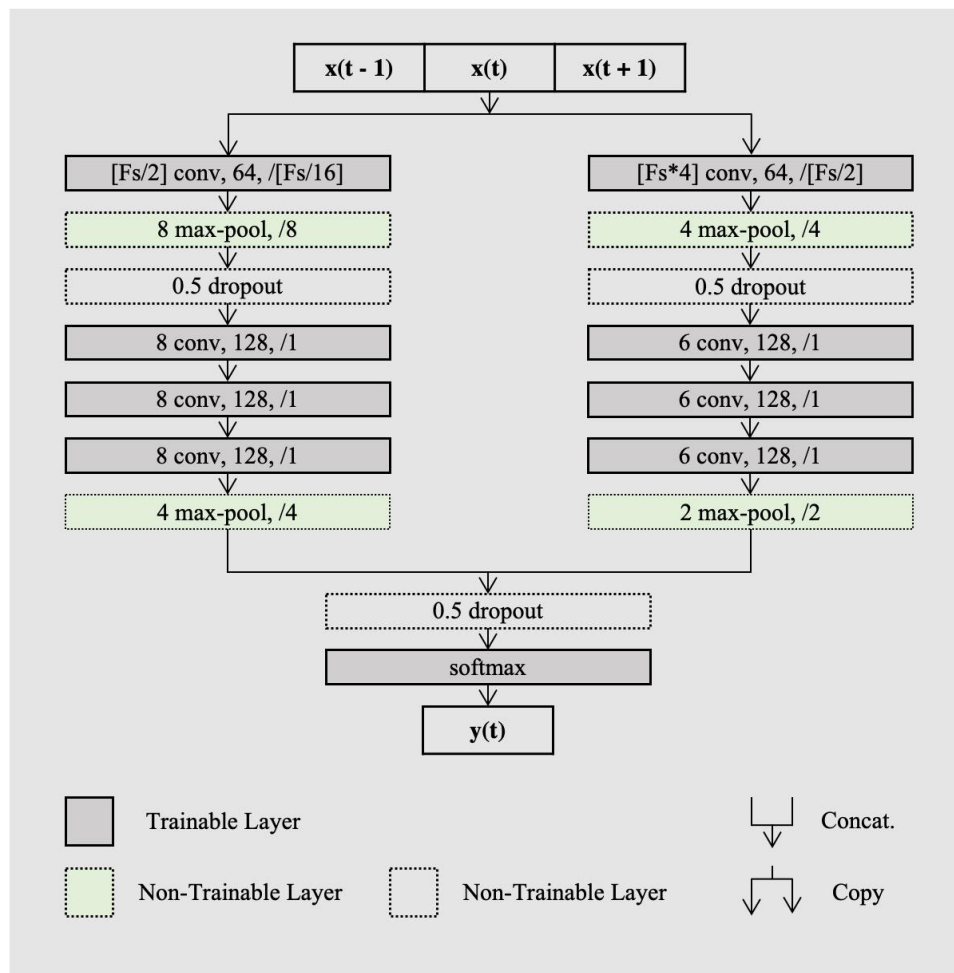


Figure 2. SimpleSleepNet architecture.

An overview of the SimpleSleepNet architecture from [23]. h_{t-1} , h'_{t-1} represent the hidden states of the GRU layers from the previous epoch of the sequence and h_{t+1} , h'_{t+1} the hidden states of the GRU layers from the next epoch of the sequence. a_t is the embedding of the current epoch.

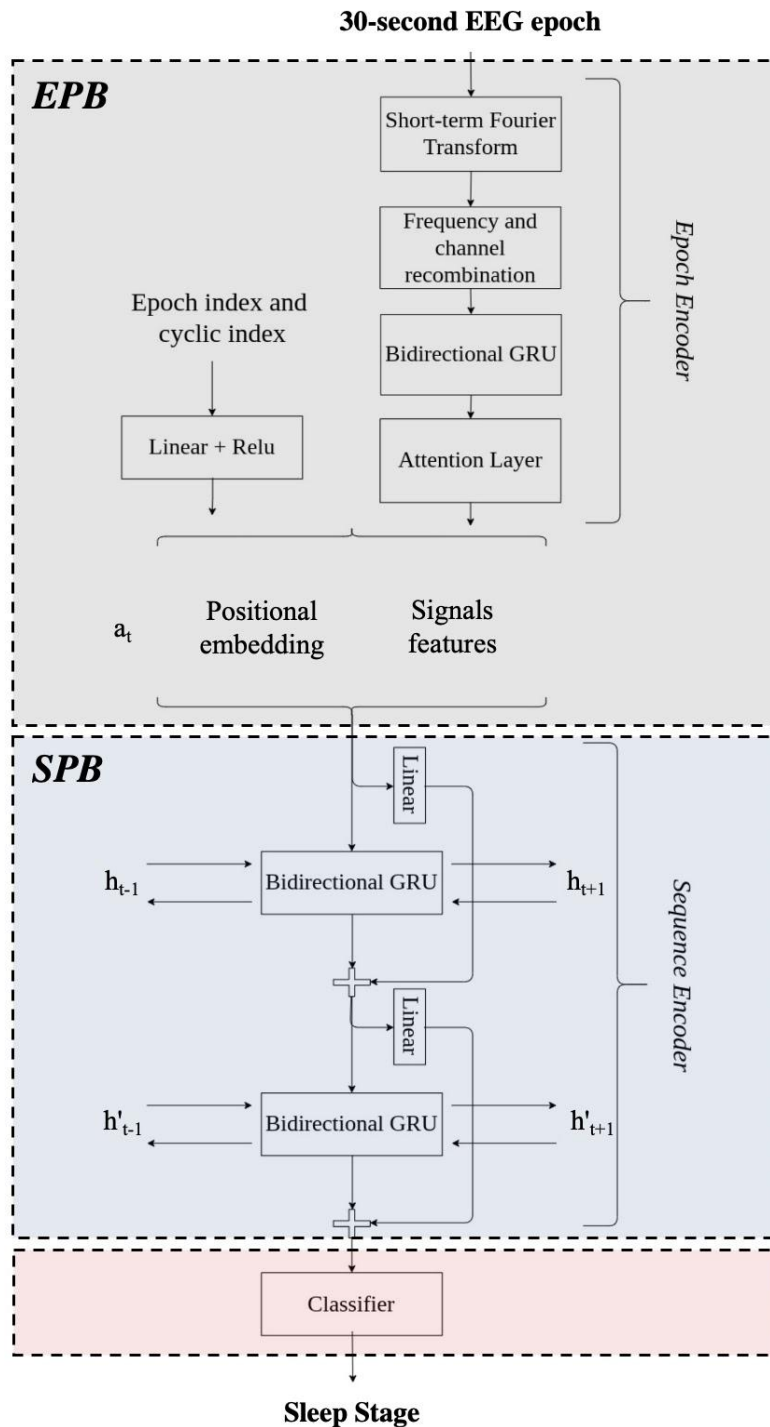
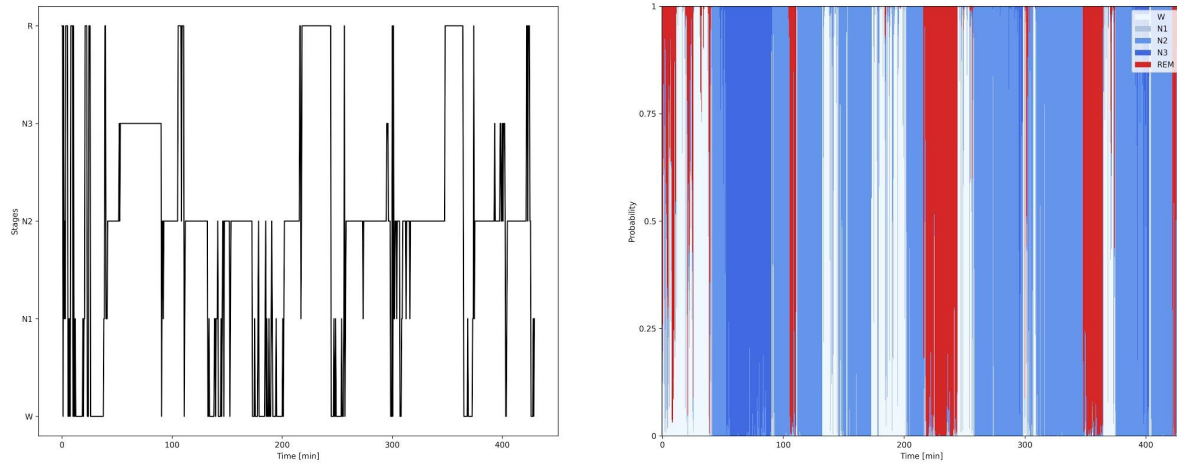


Figure 3. Hypnogram and Hypnodensity graph.

Hypnogram (left) - discrete sleep stage - and hypnodensity graph (right) - cumulative probabilities - of each sleep stage at each 30-second epoch of a patient from DOD-O.



SUPPLEMENTARY MATERIAL

Title

Multi-Scored Sleep Databases: How to Exploit the Multiple-Labels in Automated Sleep Scoring

Luigi Fiorillo^{1,2,*†}, Davide Pedroncelli^{3,†}, Valentina Agostini³, Paolo Favaro¹ and Francesca Dalia Faraci²

¹Institute of Informatics, University of Bern, Bern, Switzerland, ²Institute of Digital Technologies for Personalized Healthcare (MeDiTech), Department of Innovative Technologies, University of Applied Sciences and Arts of Southern Switzerland, Lugano, Switzerland, ³Department of Electronics and Telecommunications, Politecnico di Torino, Torino, Italy.

Institution where work was performed: Institute of Digital Technologies for Personalized Healthcare (MeDiTech), Department of Innovative Technologies, University of Applied Sciences and Arts of Southern Switzerland, Lugano, Switzerland.

†These authors contributed equally to this work.

*Corresponding author. Luigi Fiorillo, Institute of Digital Technologies for Personalized Healthcare (MeDiTech), Department of Innovative Technologies, University of Applied Sciences and Arts of Southern Switzerland, Lugano, Switzerland. Email:

luigi.fiorillo@supsi.ch.

SUPPLEMENTARY FIGURES

Figure S1. ACS across α values on DeepSleepNet-Lite.

ACS values across all the experimented α values, on both the $base+LS_U$ and the $base+LS_{Sc}$

DeepSleepNet-Lite based models tested on IS-RC, DOD-H and DOD-O datasets.

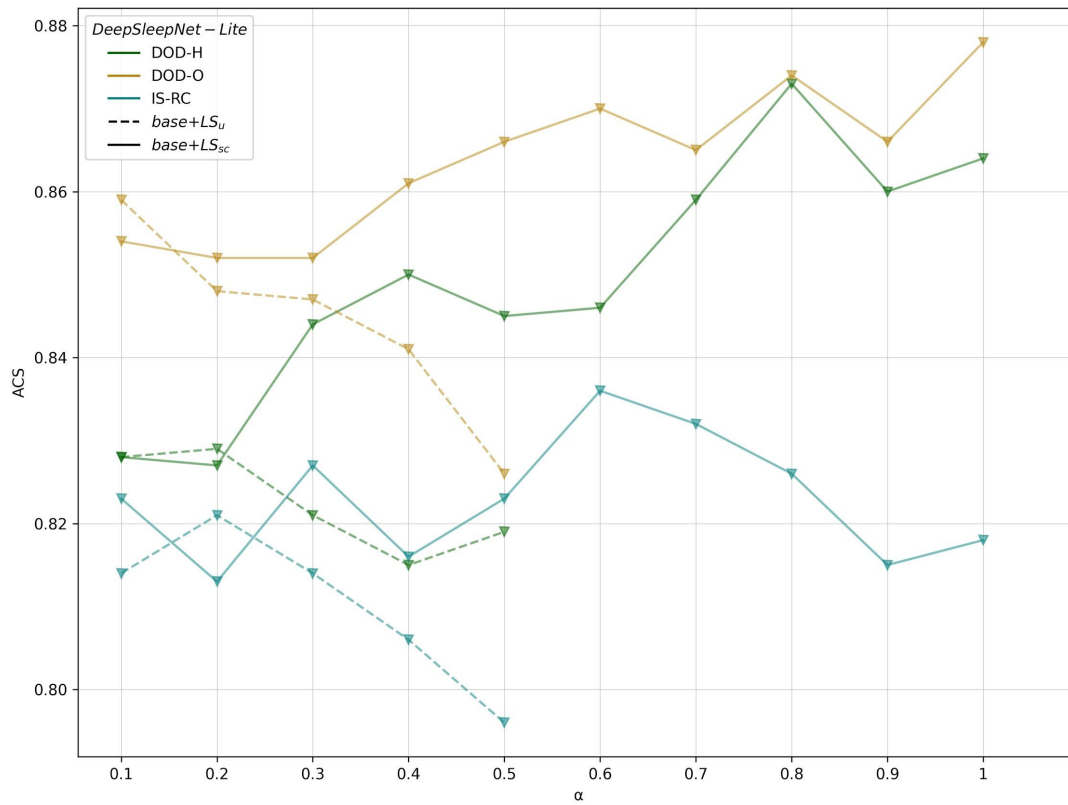
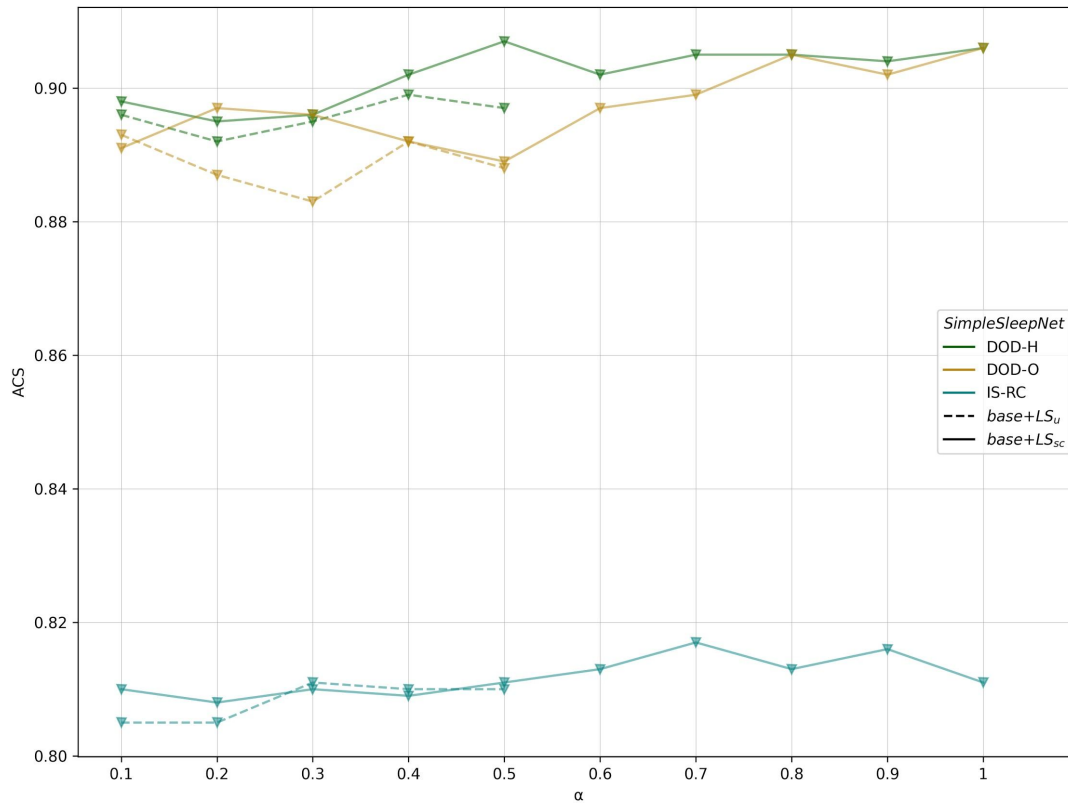


Figure S2. ACS across α values on SimpleSleepNet.

ACS values across all the experimented α values, on both the $base+LS_U$ and the $base+LS_{SC}$ SimpleSleepNet based models tested on IS-RC, DOD-H and DOD-O datasets.



SUPPLEMENTARY TABLES

Table S1. Overall performance of the DeepSleepNet-Lite models on IS-RC, DOD-H and DOD-O datasets. The metrics refer to the epochs kept after the $\mathit{argmax}(\hat{p}_{i,k})$ query selection procedures ($q\%$ threshold value fixed to 5%). We report the overall accuracy (%Acc.), macro F1-score (%MF1), Cohen’s Kappa (k), weighted-averaging F1-score (%F1) and percentage of misclassified epochs among the rejected (%miscl.). The best performance metrics for each dataset are indicated in bold.

Dataset	Models	α	Overall Metrics				%miscl.
			Acc.	MF1	k	F1	
IS-RC	base	-	79.2	69.6	0.69	79.7	56.7
	base+LS _U	0.4	79.4	69.9	0.70	80.0	58.6
	base+LS _{SC}	0.6	81.6	72.0	0.72	82.0	60.2
DOD-H	base	-	78.6	71.6	0.70	78.8	54.4
	base+LS _U	0.2	76.9	70.2	0.68	76.7	55.1
	base+LS _{SC}	0.8	82.1	74.3	0.74	82.3	56.1
DOD-O	base	-	71.2	51.7	0.58	71.6	60.4
	base+LS _U	0.1	76.6	57.8	0.65	77.5	57.6
	base+LS _{SC}	1	77.7	57.4	0.66	77.9	59.5